Springer

KSME

Journal of Mechanical Science and Technology 24 (2010) 153~158
www.springerlink.com/content/1738-494x
DOI 10.1007/s12206-009-1120-y

[Invited Paper]

Airbag tool polishing for aspherical glass lens molds †

Hocheol Lee*, Junguk Kim and Hyunhyung Kang

Department of Mechanical Engineering, Hanbat National University, Daejeon, 305-719, Korea

(Manuscript Received May 2, 2009; Revised September 30, 2009; Accepted October 12, 2009)

Abstract

This paper presents a novel airbag tool polishing technique for small aspherical glass lens molds. For a mold material such as tungsten-carbide, an ultra-precise grinding technique is used to generate the aspherical surface. However, the residual tool marks of the spiral pattern and scratch unavoidably develop on the mold surface. Therefore, post-polishing is required to obtain the optical surface. Footprinting by the superposition method without trajectory control was applied to polish the finely ground aspherical lens mold. A white light interferometer confirmed the tool mark removal effect. The final surface roughness was Ra 2nm. Microscopic observation also showed a cleaner surface without scratches.

Keywords: Airbag tool; Aspherical lens; Footprint; Polishing; Tool mark

1. Introduction

Unlike plastic lenses, aspherical glass lenses have thermal stability and high resolution of optical quality. They have been used in mobile phone cameras and HD-DVD products. Aspherical glass lenses in electronic devices are made via the compressive molding technique by pressing a glass gob onto the aspherical glass mold surface. Glass mold materials such as tungsten-carbide are used in an ultra-precise grinding machine to generate the aspherical shape [1-3]. However, the residual spiral patterns of the peak and scratches unavoidably develop on the surface. Manual polishing can remove the surface defects using a polishing pad and polishing abrasives. However, this results in a degradation in surface form accuracy because there is not much control in polishing time on the specific positions on the aspherical surface. A polishing process that controls the tool trajectory on the aspherical surface was shown to reduce the spiral pattern for the diamond-turned surface of an aspherical lens mold of nickel material [4]. It used a fixed spherical shape of a polyurethane tool and a dedicated and complex dwell time algorithm to calculate the local polishing time in a specific position. Most grounded mold surfaces already have a level of submicron form accuracy in their aspherical profile. The post-polishing process is concerned with tool mark removal in uniform polishing instead of form correction of surface profile changes. Thus, a more convenient polishing technique is required without any tool position control and trajectory calculation. An airbag polishing technique with eccentric motion has been suggested to reduce the number of polishing tool fixtures in the ophthalmic lens mold of spherical surfaces [5]. This full contact polishing mechanism has also been suggested to polish aspherical glass lens molds using both an airbag polishing tool and eccentric motion [6]. For only rough-ground molds of aspherical surfaces, experiments using one-step contact polishing showed form accuracy change of 30 percent and higher. This indicates that more studies on polishing mechanisms are necessary to prevent form changes to the aspherical profile.

2. Aspherical lens mold polishing machine

2.1 Full contact polishing mechanism

Versatile polishing kinematics has been used in the polishing process [7-8]. Conventionally, the sweep motion-based polishing process has been well established for spherical and even large optics [9]. In small and deep aspherical lens molds, tools and workpieces are arranged in reverse position, and a smaller-sized polishing tool is needed on the workpiece surface.

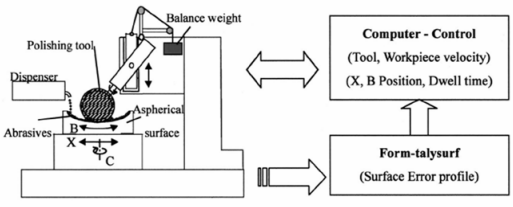

Fig. 1. Schematic diagram of the small tool polishing of aspherical lenses.

† This paper was presented at the ICMDT 2009, Jeju, Korea, June 2009. This paper was recommended for publication in revised form by Guest Editors Sung-Lim Ko, Keiichi Watanuki.

*Corresponding author. Tel.: +82 42 821 1087, Fax.: +82 42 821 1587
E-mail address: hclee@hanbat.ac.kr

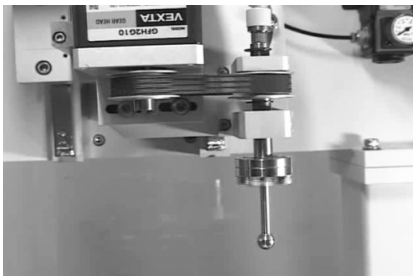

Fig. 2. Hollow spindle for an airbag polishing tool.

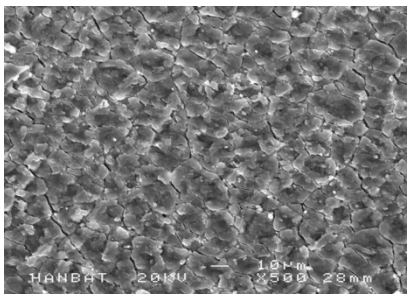

Fig. 3. Expandable pad surface of a thin rubber sheet.

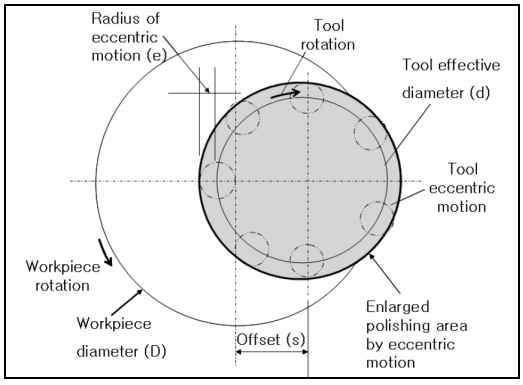

Fig. 4. The configuration of three polishing motions.

This type of small tool polishing method has been used to pol ish aspherical lens surfaces as shown in Fig. 1 [4]. All tool positions (X, B) are calculated in advance, and movements are simultaneously controlled.

In this paper, the polishing tool was replaced by an airbag tool in the above small tool polishing mechanism for full contact polishing without any kind of tool trajectory control. The tool spindle consists of a hollow shaft, and air is fed into the ball shape of the tool as shown in Fig. 2.

The pad is made of a kind of a thin rubber sheet of irregular surface structure to hold abrasives onto the surface by a scanning electron microscope as shown in Fig. 3. The pad wraps around the ball shape of the tool shaft to make an airbag. Thus, the airbag tool is expandable and comes into full contact with the surface of the rotating mold.

2.2 The configuration of three polishing motions

Three polishing motions are used in this polishing machine: eccentric motion, workpiece rotation, and tool rotation. Eccentric motion, sometimes called orbital motion, has been widely used in the ophthalmic lens process. The tool is located in the offset position and facilitates the polishing of the workpiece via the contact area of the tool's effective diameter. The eccentric motion by itself makes a uniform polishing rate on the surface. Two different abrasive motions, workpiece and tool rotations, have also been added. The configuration of the polishing motion is shown in Fig. 4. The polishing machine was constructed based on the airbag tool and three polishing motions as shown in Fig. 5. The controller makes a repetitive eccentric motion via circular interpolation of the two axes, in addition to two constant speed rotations.

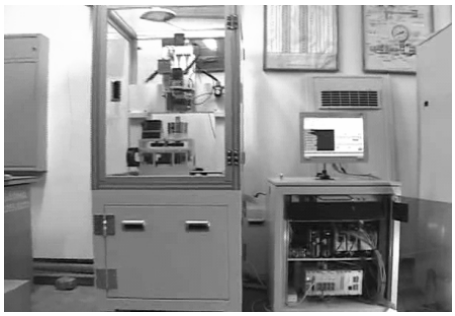

Fig. 5. Aspherical lens mold polishing machine.

3. Polishing experiment on the aspherical glass lens mold

3.1 Polishing rate

The distribution of the polishing rate in the polishing region is described in the Preston equation via multiplication of the polishing pressure (***P***) and relative velocity (***V***) distribution as shown in Eq. (1) [10]. K denotes the polishing coefficient from the abrasive type, workpiece material, and so on. In the polishing region, the velocity distribution by polishing motion is expressed with Eq. (2). The tool rotation (w), workpiece rotation (Ω), eccentric offset position (s), and constant feedrate (f) follow the circular path (e) around the eccentric offset position in Fig. 4.

$$\frac{dh}{dt} = kPV \tag{1}$$

$$V = r\varpi - (r - s)\Omega + ef \tag{2}$$

where r denotes the position in the polishing region from the origin of the axis-symmetric aspherical lens mold. All abrasives under polishing pressure move in three ways: two rotations and the eccentric motion. This is expected to deliver a polishing action with a reduced spiral peak in the grinding process. The air bag comes into full contact with the surface during all movements. The polishing pressure also remains constant regardless of the polishing movement. The pressure distribution is expected to be that of a bell shape, taking from the Hertz contact theory.

Table 1. Experiment conditions for the footprints.

Parameter		Value
Polishing load (*gf*)		310
Air pressure (MPa)		0.1
Tool diameter (mm)		8
Tool rotation speed (rpm)		80 (clockwise)
Workpiece rotation speed (rpm)		80 (counterclockwise)
Abrasives		diamond 1um
Polishing time (min)		10, 20
Tool eccentric motion (rotation)	Radius (mm)	0, 1, 2
	Federate (mm/min)	300
	Offset (mm)	0, 2, 4

Table 2. Experimental orders to obtain the footprint from the oxide wafer.

No.	Radius of eccentric motion (mm)	Offset (mm)	Polishing time (min)
1	0	0	10
2	1	0	10
3	2	0	10
4	0	2	10
5	1	2	10
6	2	2	10
7	0	4	10
8	1	4	10
9	2	4	10
10	0	0	20
11	1	0	20
12	2	0	20
13	0	2	20
14	1	2	20
15	2	2	20
16	0	4	20
17	1	4	20
18	2	4	20

3.2 Acquisition of footprint by the experimental method

To obtain the footprint or polishing pattern from Eq. (1), the experimental method was suggested using an oxide-coated silicon wafer. The ellisometer measurement of oxide thickness change guarantees the easy obtainment of the footprint on a flat surface. The initial coated oxide thickness was set to 700nm. Using the experimental conditions in Table 1, several polishing patterns are shown from Fig. 6 to Fig. 14. The pattern reflects the multiplication of airbag pressure and velocity distribution.

The polished profile of Fig. 6, Fig. 7, and Fig. 8 shows the results of three polishing experiments, where the offset was fixed to 0mm, and the radius of eccentric motion was increased from 0 to 2mm at an interval of 1mm. In all figures, the change in polishing time from 10 to 20minutes increased

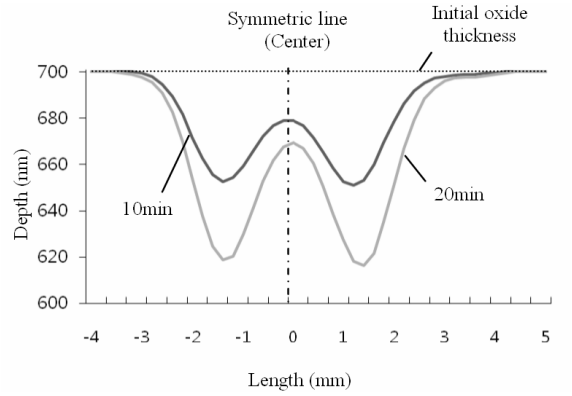

Fig. 6. Footprint of offset 0 and radius 0 (No. 1 and No. 10).

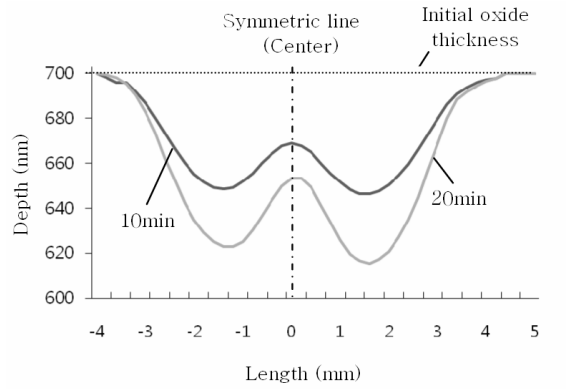

Fig. 7. Footprint of offset 0 and radius 1 (No. 2 and No. 11).

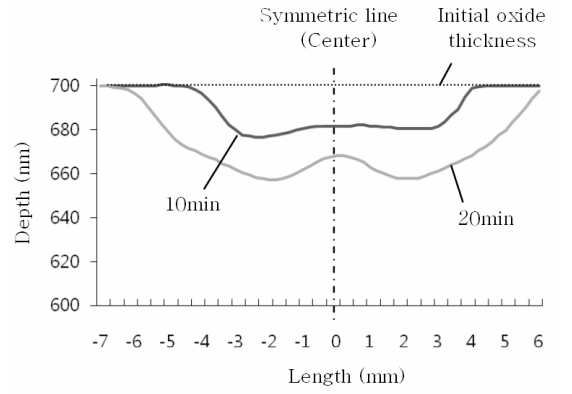

Fig. 8. Footprint of offset 0 and radius 2 (No. 3 and No. 12).

the polishing depth regardless of the radius of eccentric motion and the offset values. The pattern of footprints is shown from -3 to 3mm in Fig. 6. The central area shows the effect of the polishing pressure and the eccentric motion because the workpiece and tool rotational speeds were zero. The relative speed is at its maximum at the edge. The depth of the footprints is at its deepest around 1.5mm. Fig. 7 shows the polishing profiles when the offset was fixed to 0mm, and the radius of eccentric motion was 1mm. All shape characteristics are similar to Fig. 6. However, a relatively larger area was polished by the change in radius of eccentric motion. The radius

of eccentric motion was increased to 2mm in Fig. 8. The bump in the central area became smaller, and the flat polishing profile appeared except at the edges. The peak polishing rates in Fig. 6 and Fig. 7 were about 50nm at 10minutes and 80nm at 20minutes, respectively. The polishing rate does not appear to be linearly dependent on polishing time. The peak polishing rates in Fig. 8 at the radius of 2mm were about 20nm at 10minutes and 50nm at 20minutes.

The polish profiles of Fig. 9, Fig. 10, and Fig. 11 show the results of three polishing experiments, where the offset was fixed to 2mm, and the radius of eccentric motion was increased from 0 to 2mm in intervals of 1mm. The width of the bump in the central region was increased by a change in offset position. The footprints are only shown as expanded shapes of the footprints in the offset position of 0mm. The widths of the footprints in Fig. 11 were enlarged to about 14mm.

The footprints of Fig. 12, Fig. 13, Fig. 14 have the offset position of 4mm. The radius of eccentric motion also increased from 0 to 2mm in intervals of 1mm. In Fig. 12 and Fig. 13, the small radius of eccentric motion under a large offset caused no polishing region in the footprints. The increased radius of eccentric motion at 2mm shows just a slight polishing effect in the central polishing area. The widths of the footprints in Fig. 14 were enlarged to about 19mm.

Finally, two footprints were experimentally superimposed on the same oxide coated wafer to obtain a wider flat footprint on the polishing region, considering the effective diameter of the spherical lens mold. The two footprints of Fig. 8 and Fig.

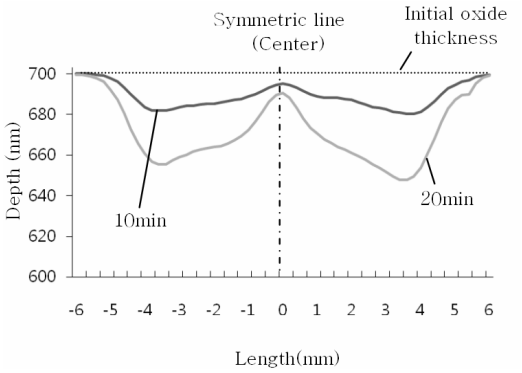

Fig. 9. Footprint of offset 2 and radius 0 (No. 4 and No. 13).

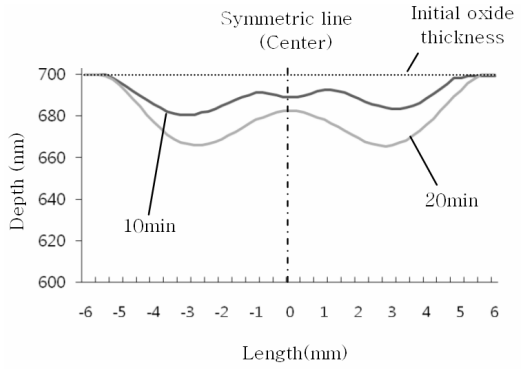

Fig. 10. Footprint of offset 2 and radius 1 (No. 5 and No. 14).

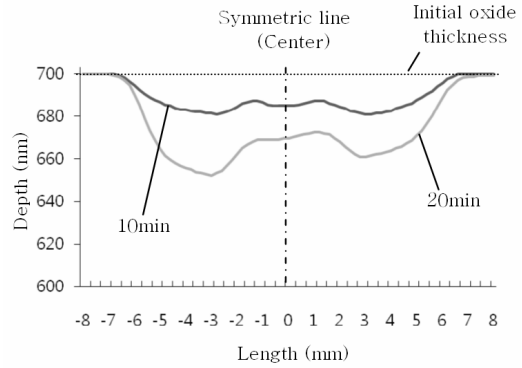

Fig. 11. Footprint of offset 2 and radius 2 (No. 6 and No. 15).

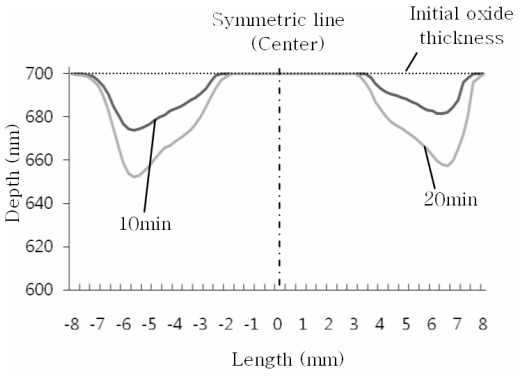

Fig. 12. Footprint of offset 4 and radius 0 (No. 7 and No. 16).

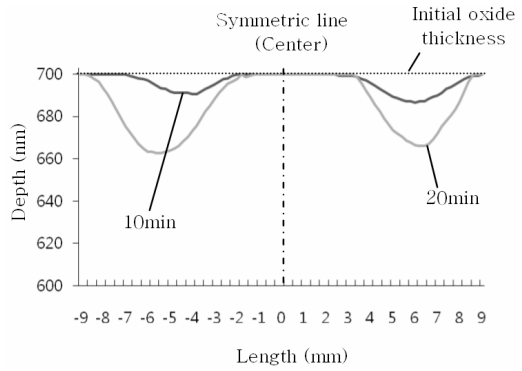

Fig. 13. Footprint of offset 4 and radius 1 (No. 8 and No. 17).

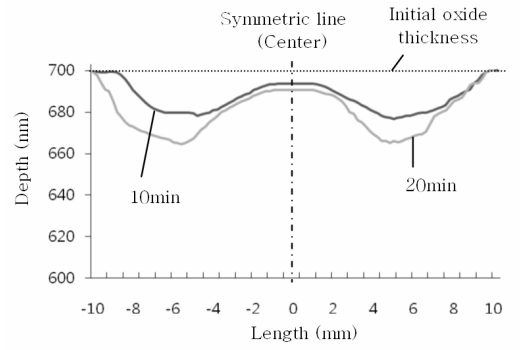

Fig. 14. Footprint of offset 4 and radius 2 (No. 9 and No. 18).

Table 3. Experimental conditions for the superposition of two offset footprints on an oxide-coated wafer.

Parameter		1st	2nd
Polishing load (*gf*)		310	
Air pressure (MPa)		0.1	
Tool diameter (mm)		8	
Tool rotation speed (rpm)		80 (clockwise)	
Workpiece rotation speed (rpm)		80 (counterclockwise)	
Abrasives		diamond 1um	
Tool eccentric motion (rotation)	Radius (mm)	2	
	Offset (mm)	0	2
Polishing Time (min)		20	15

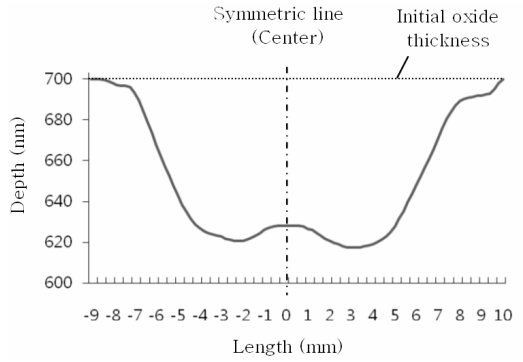

Fig. 15. Footprint from the superposition of two offset positions 2 (No. 8 and No. 11).

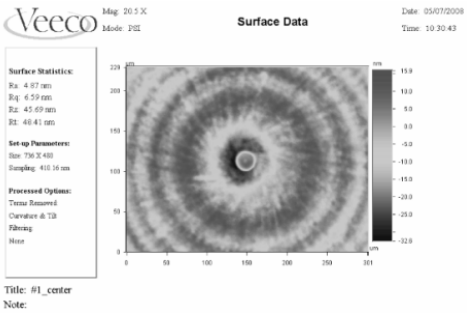

(a) Whitelight interferometer

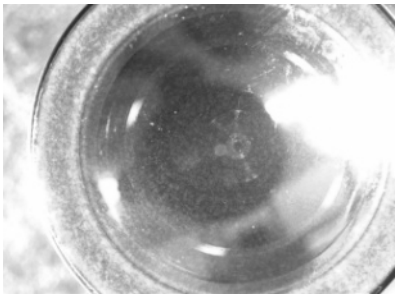

(b) Microscope

Fig. 16. Tool marks and scratches resulting from the grinding process.

11 were selected, and the polishing times were changed to 20 and 15 minutes, respectively. The new superposed footprint shows a small bump in the mold center and the edge slope.

Table 4. Surface roughness variation via airbag tool polishing.

	Rt (peak-to-valley)	Ra (average)	Rrms (root-mean-square)
Before Polishing (nm)	67.5	3.2	4.3
After Polishing (nm)	36	3.6	4.6

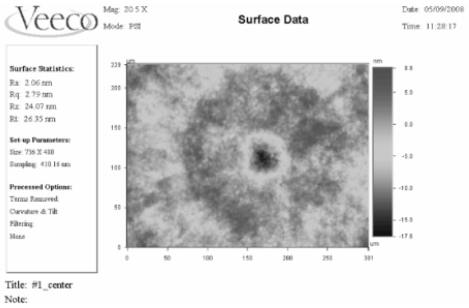

(a) Whitelight interferometer

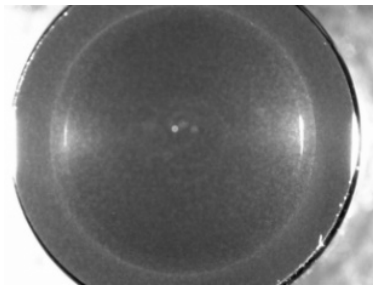

(b) Microscope

Fig. 17. Tool mark reduction after airbag tool polishing.

The pattern shows a tolerable uniform rate except at the edge. A bump located only at center can make a form change together with the edge slope. The effective polishing region would still be limited to the flat area except at the edge. The polished region should be larger than the effective area of the polished lens mold to keep the uniform rate. If an extension block surrounds the lens mold, the lens mold area would have a flat region of at least 8mm in 16mm as in Fig. 15.

3.3 Tool mark removal experiment

Tool mark removal was performed using the superimposed footprint in Fig. 15 for a fine-ground aspherical lens mold. Before polishing, a white-light interferometer and microscope measured the lens mold surface. The spiral tool marks and scratch on the surface are shown in Fig. 16. The spiral peak resulted from the grinding tool path. The surface roughness of the central area was Ra 5nm. After polishing using the superimposed footprint, the surface roughness was improved to Ra 2nm.

Tool marks were also removed, and the surface was cleaned as shown in Fig. 17. Formtalysurf measured another level of surface roughness as shown in Table 4. The surface roughness was improved from Rt (Peak-to-Valley) 67.5nm to 36nm. Form error measurements by Formtalysurf showed a slight change in the aspherical lens profile as shown in Fig. 18.

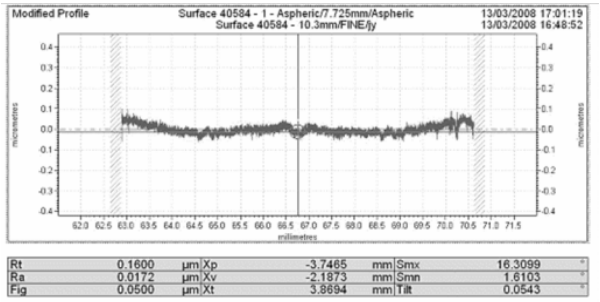

(a) Before polishing

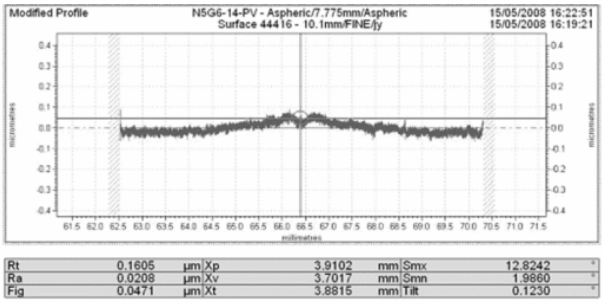

(b) After polishing

Fig. 18. Form error profile via airbag tool polishing.

During the polishing process, the form error level of Rt 0.16um was maintained.

4. Conclusions

For the polishing of finely ground aspherical lens molds, the airbag polishing technique is suggested. A polishing machine was constructed using an airbag tool and three polishing motions. The superposition method of the footprint of the polishing pattern was introduced to obtain extended full-contact polishing without needing to consider aspherical lens profiles or tool trajectory controls. Tool mark removal experiments showed an improvement in the optical surface quality of the lens mold. The form error level was maintained during the airbag tool polishing process.

Acknowledgment

This research was supported by the Basic Science Research Program through the National Research Foundation of Korea (NRF) funded by the Ministry of Education, Science, and Technology (Grant No. 2009-0059393).

References

[1] H. Suzuki and T. Komiyama, Precision grinding of molding die and glass molding in micro optical components, *Proc. 9th International Conference for Production Engineering*, Osaka, Japan (1999) 126-131.

[2] W. B. Lee, C. F. Cheung, W. M. Chiu and T. P. Leung, An investigation of residual form error compensation in the ultra-precision machining of aspheric surfaces, *Journal of Materials Processing Technology*, 99 (1-3), (2000) 129-134.

[3] J. Lee, M. Saeki, T. Kuriyagawa and K. Syoji, A study on the mirror grinding for mold of a small aspherical lens, *International Journal the Korean Society of Precision Engineering*, 4 (3), (2003) 48-54.

[4] H. Lee and M. Yang, 2001, Dwell time algorithm for computer controlled polishing of small axis-symmetrical aspherical lens mold, *Optical Engineering*, 40 (9) (2001) 1936-1943.

[5] H. Lee, A study on optics polishing technology by adaptive tool and eccentric motion mechanism, *Journal of Korea Society of Machine Tool Engineers*, 16 (6) (2007), 133-139.

[6] H. Lee and J. Kim, Full contact polishing method of aspherical glass lens mold by airbag polishing tool, *Journal of Korea Society of Machine Tool Engineers*, 17 (5) (2008) 82-88.

[7] H. Suzuki, T. Moriwaki, T. Okino and Y. Ando, Development of ultrasonic vibration assisted polishing machine for micro aspheric die and mold, *CIRP Annals - Manufacturing Technology*, 55 (1) (2006) 385-388.

[8] G. Doughty and J. Smith, Microcomputer-controlled polishing machine for very smooth and deep aspherical surfaces, *Applied Optics*, 26 (12) (1987) 2421-2426.

[9] H. Karow, *Fabrication Methods for Precision Optics*, John Wiley & Sones, Inc., (2004) 342-351.

[10] M. Yang and H. Lee, Local material removal mechanism considering curvature effect in the polishing process of the small aspherical lens die, *Journal of Materials processing technology*, 116 (2001) 298-304.

Hocheol Lee received his B.S. and M.S degrees in Mechanical Engineering from Seoul National University, Korea, in 1988 and 1990, respectively. He then received his Ph.D. degree from the Korea Advanced Institute of Science and Technology in 2000. Dr. Lee is currently a professor at the School of Mechanical Engineering at Hanbat National University in Daejeon, Korea. He has worked with Samsung Electronics Co., Boston University, and the National Institute of Standard and Technology in USA. Dr. Lee's research interests include optics manufacturing process and system, optical surface design, and micro-machining.